Journal of Applied Fluid Mechanics, Vol. 17, No. 1, pp. 75-88, 2024.
Available online at www.jafmonline.net, ISSN 1735-3572, EISSN 1735-3645.
https://doi.org/10.47176/jafm.17.1.2061

Numerical Simulation of Crude Oil Leakage from Damaged Submarine-Buried Pipeline

H. J. Zhao, D. Zhang, X. F. Lv†, L. L. Song, J. W. Li, F. Chen and X. Q. Xie

Jiangsu Key Laboratory of Oil and Gas Storage and Transportation Technology, Changzhou University, Changzhou, Jiangsu Province, 213100, China
School of Petroleum and Natural Gas Engineering, Changzhou University, Changzhou, Jiangsu Province, 213100, China

†Corresponding Author Email: lvxf@cczu.edu.cn

ABSTRACT

Oil spill accidents in damaged submarine-buried pipelines cause tremendous economic losses and serious environmental pollution. The accurate prediction of oil spills from subsea pipelines is important for emergency response. In this study, the volume-of-fluid model, realizable k–ε turbulence model, and porous-medium model were employed to describe the process of an oil spill from a submarine pipeline to the sea surface. The effects of seawater density, seawater velocity, and pipeline buried depth on the transverse diffusion distance of crude oil and the time at which crude oil reaches the sea surface were obtained through numerical calculations. The calculation results show that, with a decrease in seawater density and an increase in seawater velocity and pipeline depth, the diffusion rate of crude oil decreases significantly, the maximum transverse diffusion distance increases and crude oil takes a long time to reach the sea surface. In particular, compared with a sea density of 1045 kg/m^3, the transverse distance of a sea density of 1025 kg/m^3 is increased by 0.091 m. When the seawater velocity is greater than 1.5 m/s, the diffusion of crude oil in seawater is significantly affected, the seawater velocity increases to 0.35 m/s, and the transverse diffusion distance of oil to the sea surface increases to 12.693 m. When the buried depth of the pipeline reaches 0.7 and 1.3 m compared to 0.1 m, the diffusion widths of crude oil in sea mud rise by 20% and 32.5%, respectively. The time required for crude oil to reach the sea surface and the transverse diffusion distance of crude oil migrating to the sea surface were analyzed using multiple regression, and the fitting formulas were obtained. The results provide theoretical support for accurately predicting the leakage range of submarine-buried pipelines and provide valuable guidance for submarine-buried pipeline leakage accident treatment schemes.

Article History

Received June 1, 2023
Revised August 10, 2023
Accepted August 24, 2023
Available online November 1, 2023

Keywords:

Submarine buried pipeline
Crude oil leakage
Oil spill
Numerical simulation
Multiphase flow

1. INTRODUCTION

Offshore oil and gas pipelines are critical for delivering oil and gas products. The leakage of a submarine oil pipeline causes extensive damage to the marine environment, human health, and natural resources. Severe leakage accidents can lead to unpredictable economic losses (Mark et al., 2004; Wei et al., 2018; Zhang et al., 2022). When a submarine crude oil leak occurs, it is necessary to take measures to reduce the harm as soon as possible. Accurately predicting the leakage and oil spill processes of submarine-buried crude oil pipelines is of great significance for emergency response.

Research on submarine crude oil pipeline leakage has mainly focused on two subjects: the diffusion process in seawater and the diffusion process in sea mud (Yang et al., 2016). Regarding the diffusion of crude oil in seawater, Wang et al. (2018) used computational fluid dynamics (CFD) to simulate the jet situation of crude oil leakage with different flow rates. The results showed that, when the water flow rate was high, the position of the jet was low, and the lateral displacement of the oil leakage was first slowly diffused and then accelerated. Liu (2015) used

NOMENCLATURE

$C_{1\varepsilon}$	constant	u_w	velocity of seawater at depth
c_2	inertia loss coefficient	u_{wmax}	maximum velocity of seawater
C_2	constant	y_w	current depth of seawater
$C_{3\varepsilon}$	constant	η	relative strain parameter
$C\mu$	constant	σ_ε	turbulent Prandtl number
Dp	particle diameter of porous media	σ_t	turbulent Prandtl number
G_b	turbulence kinetic energy	α	permeability of porous media
G_k	turbulence kinetic energy generated	α_q	volume fraction of q phase
H	total depth of seawater	ε	porosity ratio of porous media
k	turbulence kinetic energy	μ	hydrodynamic viscosity
p	pressure	μ_t	turbulent viscosity
Pr_t	Prandtl number	ρ	density of oil-water mixture
S	strain rate	ρ_q	q phase density
u_{qi}	velocity in i direction		

the finite volume method and PISO algorithm to simulate the effects of different jet velocities and leakage apertures on the leakage of submarine crude oil pipelines. The results showed that, with an increase in the leakage aperture and jet velocity, the oil column injected at the same time is longer, the time to reach sea level is shorter, and the pollution range is larger. Zhu et al. (2014, 2017a) studied the process of oil spill to a free surface with different leak sizes and investigated the effects of crude oil density, oil leakage rate, oil leakage amount, and seawater velocity on the leakage process, by analyzing the time it took for oil droplets to reach the sea surface and the migration distance in the direction of coastal water velocity. Sun et al. (2019) simulated the diffusion process of underwater oil spills and oil spills after they reached the sea surface using a two-dimensional numerical model, and they analyzed the influence of wave wavelength, seawater velocity, wind velocity, leakage direction, crude oil density, and leakage rate on oil spill diffusion.

To study the diffusion of crude oil in sea mud, Liu et al. (2012) simulated the temperature field and pressure field in the sea mud during hot oil leakage using a porous-medium coupling model. The simulation results showed that the temperature of the sea mud around the pipeline fluctuates violently within a certain period after the pipeline leaked. The temperature of the crude oil in the leakage front dropped rapidly, and the range of the heat-affected zone gradually stabilized. Shi et al. (2014) established the mathematical model of crude oil pipeline leakage in water by using the VOF model and studied the influence of the crude oil leakage velocity and water flow velocity on the leakage law. The simulation results showed that the crude oil leakage velocity and water flow velocity are positively correlated with the oil leakage range. Guan et al. (2015) studied the influences of seawater velocity and leakage hole direction on the oil leakage and diffusion characteristics of submarine pipelines. The simulation results showed that, when the leakage direction is 45 ° to the countercurrent direction of seawater, the crude oil diffusion leakage is very intense.

Most studies on the leakage of submarine crude oil pipelines have focused on the diffusion of crude oil in seawater (Han et al., 2015; He et al., 2017; Lin et al., 2017; Bonvicini et al., 2018; Ji et al., 2018; Kotzakoulakis & George 2018; Lu et al., 2018; Fu et al., 2020; Gong et al., 2020). However, research on the diffusion law of crude oil in sea mud and seawater basins has been relatively scarce. In addition, experiments on crude oil leakage and diffusion in submarine-buried pipelines are costly and dangerous, whereas numerical simulations are economical and safe (Manda et al., 2020, 2021, 2022, 2023). In this study, the VOF multiphase flow model and porous-medium model were combined to establish a numerical model for the leakage of submarine-buried crude oil pipelines under the condition of sea-mud–seawater coupling. Considering the influences of seawater density, seawater velocity, and pipeline buried depth on the leakage, diffusion, and drift characteristics of crude oil, the diffusion law of crude oil after entering seawater was studied, and the migration characteristics of crude oil were obtained. Finally, through multiple linear regression analysis, formulas for the time of crude oil reaching the sea surface and the transverse diffusion distance of crude oil under the influence of seawater density, seawater velocity, and pipeline burial depth were established. The research results provide theoretical support for formulating treatment schemes for submarine-buried pipeline leakage accidents.

2. SIMULATION METHOD

2.1 Computational Domain

Figure 1 shows the simulation domain's geometry, point O is the origin of the coordinates, the x-direction is parallel to the direction of the seawater velocity, the y-direction is perpendicular to the direction of the sea surface, the z-direction is parallel to the direction of the

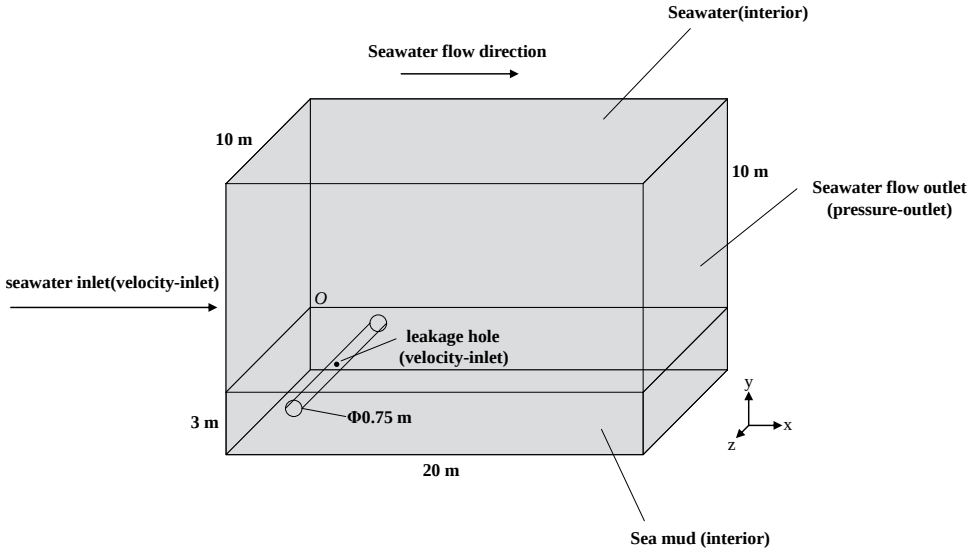

Fig. 1 Geometric model of submarine-buried crude oil pipeline

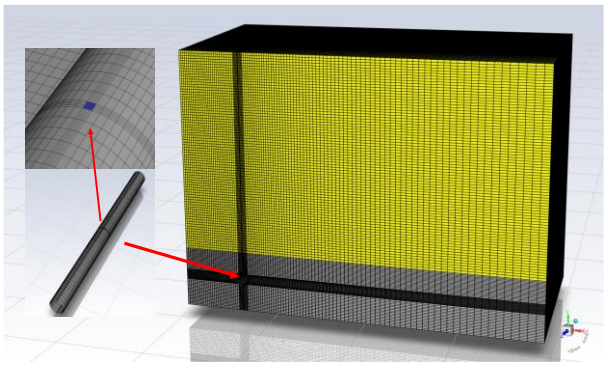

Fig. 2 Mesh of submarine-buried crude oil pipeline

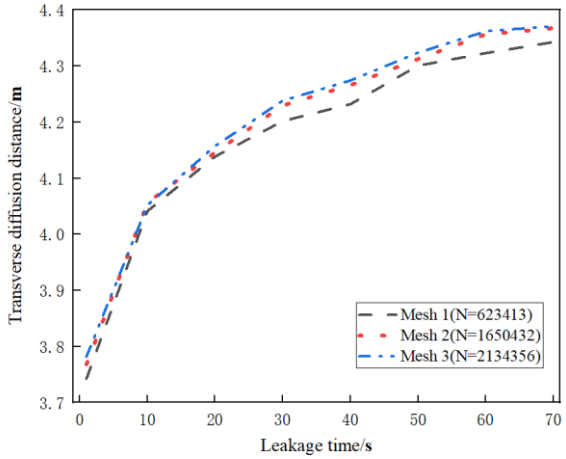

Fig. 3 Grid independence verification

fluid flow in the pipeline. The simulation domain is a hexahedron area with a length of 20 m, width of 10 m, and height of 13 m. The lower part is sea mud with a depth of 3 m, and the upper part is seawater with a depth of 10 m. The buried depth of the pipeline is 0.1 m. The length of the pipeline is 10 m, and the diameter is 0.75 m. The diameter of the leakage hole is taken as 0.045 m, which is located directly above the middle of the pipeline (z = 5 m). The transverse diffusion distance in the following represents the distance of the crude oil moving parallel to the *x*-axis with the leakage hole as the origin. The diffusion height represents the distance of the crude oil moving parallel to the *y*-axis with the leakage hole as the origin.

2.2 Mesh Generation

ICEM was used to mesh the simulation domain using a hexahedral mesh, and mesh refinement was performed at the junction of the sea mud and seawater, leak holes, and surrounding areas (Fig. 2). To ensure simulation accuracy, three groups of calculation results with different grid numbers were selected for comparison. The simulation results of the change in the transverse diffusion distance of crude oil with time were compared, and the results are shown in Fig. 3. The figure shows that Mesh 2, with cell number 1650432, can better balance the computational efficiency and result accuracy.

2.3 Governing Equation

The VOF model is suitable for the case of a gas-liquid two-phase system with a clear phase interface. Such physical phenomena as stratified flow, free surface flow, bubble flow, and dam break in real life can be calculated using the VOF model.

In this study, sea mud was regarded as a saturated water-bearing porous medium, and the diffusion of leaked crude oil in sea mud was simplified as the flow of oil and water in porous media. The VOF and porous media models were used for numerical simulation. The diffusion process of crude oil in seawater was analyzed using the VOF multiphase flow model (Neofytou et al., 2006; Papadimitrakis et al., 2006; Wols et al., 2010), and the realizable *k-ε* turbulence model was adopted. The governing equations are as follows:

The continuity equation is

$$\frac{\partial}{\partial t}\left(\alpha_q \rho_q\right)+\frac{\partial}{\partial x_i}\left(\alpha_q \rho_q u_{qi}\right)=0 \tag{1}$$

where α_q is the volume fraction of the q phase, ρ_q is q-phase density, and u_{qi} is the velocity in the i-direction.

The Momentum equation is

$$\frac{\partial}{\partial t}(\rho u_i)+\frac{\partial}{\partial x_j}(\rho u_i u_j)=-\frac{\partial p}{\partial x_i}+\mu\nabla^2 u_i+\rho g_i +F_i+\left[\frac{\mu}{\alpha}u_i+c_2\frac{1}{2}\rho|u_i|u_i\right] \tag{2}$$

$$\rho=\alpha_o\rho_o+(1-\alpha_o)\rho_w \tag{3}$$

where ρ represents the density of the oil-water mixture. The subscripts o and w represent the oil and water phases, respectively. p represents pressure. μ is the hydrodynamic viscosity.c_2 is the inertia loss coefficient. F_i represents other forces, and α is the permeability of porous media. The expression is

$$\alpha=\frac{D_p^2}{150}\cdot\frac{\varepsilon^3}{(1-\varepsilon)^2} \tag{4}$$

where ε is the porosity ratio of porous media, and $D_p$is the particle diameter of porous media.

The turbulence equations are

$$\frac{\partial(\rho k)}{\partial t}+\frac{\partial(\rho k u_i)}{\partial x_i}=\frac{\partial}{\partial x_i}\left[\left(\mu+\frac{\mu_t}{\sigma_k}\right)\frac{\partial k}{\partial x_i}\right] +G_k+G_b-\rho\varepsilon-Y_M \tag{5}$$

$$\frac{\partial(\rho\varepsilon)}{\partial t}+\frac{\partial(\rho\varepsilon u_i)}{\partial x_i}=\frac{\partial}{\partial x_j}\left[\left(\mu+\frac{\mu_t}{\sigma_\varepsilon}\right)\frac{\partial\varepsilon}{\partial x_j}\right] +\frac{\varepsilon}{k}C_{1\varepsilon}G_b\left(1-C_{3\varepsilon}\right)-C_2\rho\frac{\varepsilon^2}{k+\sqrt{\varepsilon\nu}}+\rho C_1 S\varepsilon \tag{6}$$

in which,

$$C_1=\max\left(0.43,\frac{\eta}{\eta+5}\right) \tag{7}$$

$$\eta=\frac{k}{\varepsilon}S \tag{8}$$

$$S=\sqrt{2S_{ij}S_{ij}} \tag{9}$$

$$S_{ij}=\frac{1}{2}\left(\frac{\partial u_j}{\partial x_i}+\frac{\partial u_i}{\partial x_j}\right) \tag{10}$$

$$G_k=-\rho\overline{u_i' u_j'}\frac{\partial u_j}{\partial x_i} \tag{11}$$

$$G_b=-g_i\frac{\mu_t}{Pr_t}\frac{\partial\rho}{\rho\partial x_i} \tag{12}$$

$$\mu_t=\rho C_\mu\frac{k^2}{\varepsilon} \tag{13}$$

where Y_M is the effect of the pulsating expansion on the total dissipation rate in compressible turbulence. k is turbulence kinetic energy, ε represents turbulent dissipation rate, S is the strain rate, η is the relative strain parameter, μ_t represents turbulent viscosity, σ_t and σ_ε represent the turbulent Prandtl number taken as 1.0 and 1.2, respectively, G_k is the turbulence kinetic energy generated by average velocity gradient, Pr_t is the turbulent Prandtl number taken as 0.85, G_b is the turbulence kinetic energy generated by buoyancy, and $C_{1\varepsilon}$, C_2, $C_{3\varepsilon}$ and $C_\mu$are constants taken as 1.44, 1.0, 0.9 and 0.09, respectively.

2.4 Numerical Method

In this study, ANSYS Fluent 2020R2 software was used for numerical simulation. The finite volume method was used to address the problem of crude oil leakage. The unsteady model was adopted, and the time step was defined as 0.01s. The PISO algorithm was employed to solve pressure-velocity coupling. The second-order upwind scheme discretized the momentum equation and the pressure discrete PRESTO! algorithm was selected. The Boussinesq approximation is adopted considering the buoyancy of seawater. The convergence criterion for all the calculations was set to be less than 10^{-6} residuals.

2.5 Boundary condition

The seawater velocity profile is used to express the relationship between seawater velocity and seawater depth, (Sun et al., 2019), and the modified seawater inlet condition is defined by user-defined function (UDF) programming (See Appendix). The specific formula is

$$u_w=-\frac{u_{wmax}}{H^2}\left(y_w-H\right)^2+u_{wmax} \tag{14}$$

where H is the total depth of seawater, y_w is the current depth of seawater, u_{wmax} is the maximum velocity of seawater (surface velocity of seawater), and u_w is the velocity of seawater at depth y_w.

The leakage port of the pipeline and seawater inlet are defined as “velocity-inlet”, and the seawater flow outlet is “pressure-outlet”. The pipe wall, the surrounding of sea mud, and the bottom surface of the simulation domain are defined as “wall”. In the seawater part, the side and sea surface of the simulation domain are defined as symmetry. The interface between seawater and sea mud is defined as “interior” (Fig. 1).

2.6 Model Validation

Few studies have been conducted on leakage from submarine-buried pipelines. In this study, the experimental data of small hole leakages in buried pipelines and underwater diffusion of oil spills in submarine pipelines were selected to verify the model of submarine-buried pipelines with the same experimental size.

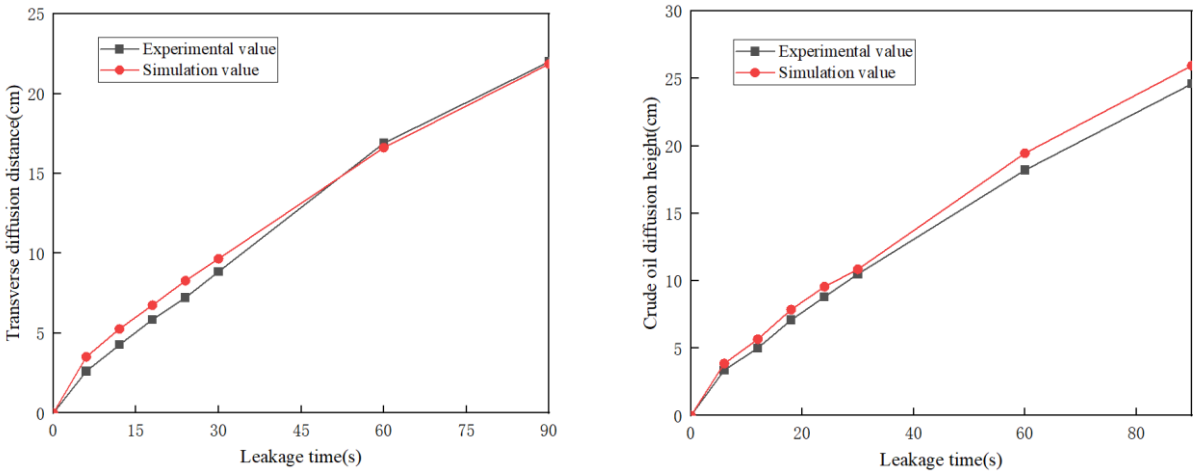

(a) Comparison of transverse diffusion distance of crude oil

(b) Comparison of crude oil diffusion height distance

Fig. 4 Comparison of experimental and simulated values

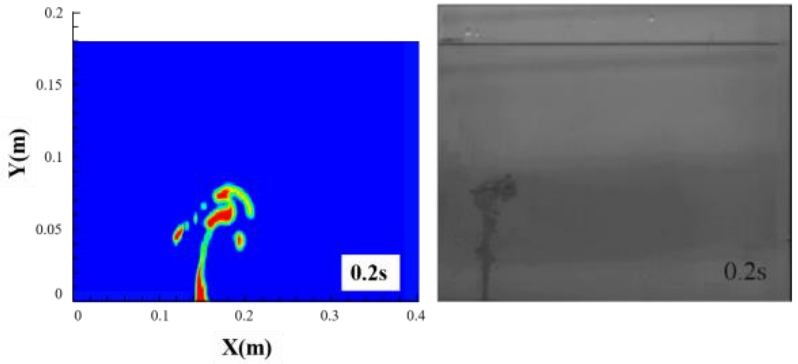

(a) t=0.2 s

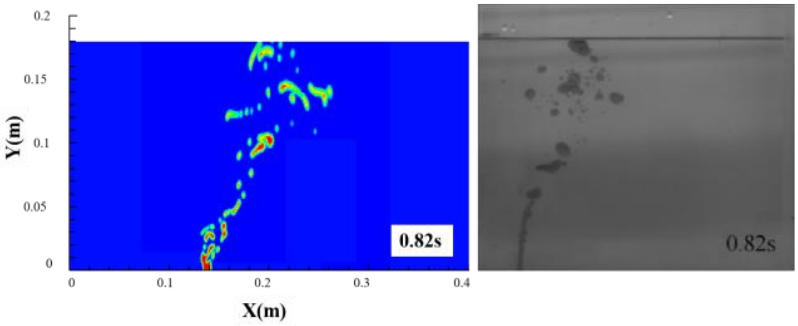

(b) t=0.82 s

Fig. 5 Comparison of oil phase distributions in the experiment and numerical simulation

Through comparison with the experimental results of Zhang et al. (2015), the accuracy of the numerical model in this study for the diffusion process of crude oil in sea mud was verified, as shown in Fig. 4. The analysis revealed that the transverse diffusion distance of crude oil and diffusion height curve of crude oil obtained by the numerical simulation were basically consistent with the experimental results. The main reason for the error is that the uniform porous-medium model was used to simulate the diffusion law of the soil. The error is relatively small. Therefore, the numerical model established in this study has a high calculation accuracy in simulating porous media, such as soil sea mud.

The accuracy of the numerical model for seawater was verified through a comparison with the experimental results of Zhu et al. (2017b). When numerical simulation was conducted, the leakage pressure was defined as 99 hPa, and the distribution patterns of oil products when the experimental times were 0.2 s and 0.82 s respectively are compared with the crude oil phase distribution diagram in the simulation results at the same time, as shown in Fig. 5. In comparison, the diffusion patterns of crude oil in seawater were similar at the same times, and the scope was

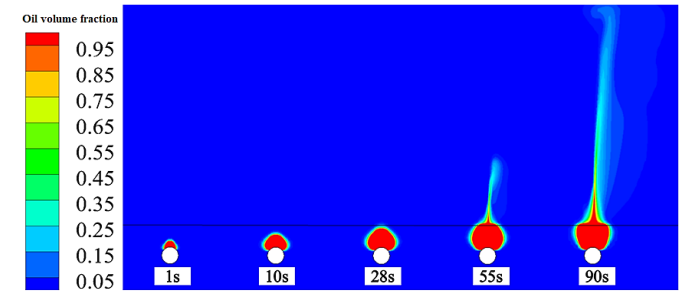

(a) ρ_w =1025 kg/m^3

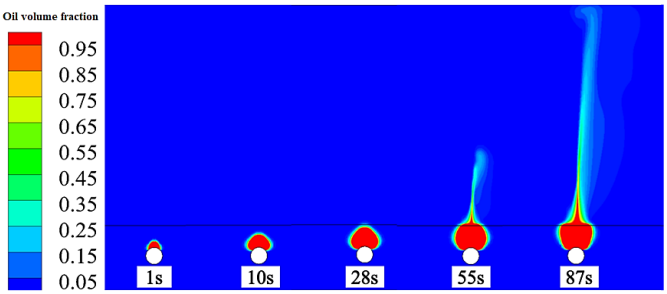

(b) ρ_w =1035 kg/m^3

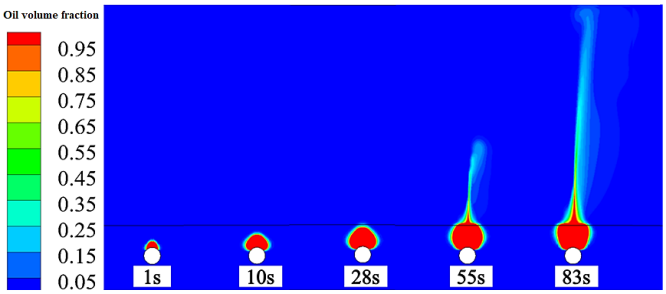

(c) ρ_w =1045 kg/m^3

Fig. 6 Crude oil volume fraction at different seawater densities

Table 1 Simulation cases

Case	Seawater density (kg/m^3)	Seawater velocity (m/s)	Buried depth of pipeline (m)
1	1025	0.05	1
2	1035	0.05	1
3	1045	0.05	1
4	1025	0.05	0.1
5	1025	0.1	0.1
6	1025	0.15	0.1
7	1025	0.25	0.1
8	1025	0.35	0.1
9	1025	0.05	0.7
10	1025	0.05	1.3

roughly the same. It was confirmed that the established model could accurately simulate the diffusion process of crude oil in seawater.

3. RESULTS AND DISCUSSIONS

When a submarine-buried pipeline leaks, it is affected by pipeline parameters and the marine environment. In this study, considering that there are different seawater densities, seawater velocities, and seabed sediments in different sea areas, the gradual loss of seabed sediment under the erosion of water flow leads to a change in the pipeline buried depth. Three factors (seawater density, seawater velocities, and pipeline buried depth) were studied to explore the diffusion law of submarine-buried crude oil pipelines. The parameters of the simulation in this study were primarily based on the development report of an oilfield group in the Bohai Sea, China. The 10 simulation cases are listed in Table 1.

3.1 Seawater Density

The buried depth of the pipeline h was taken as 1 m, and the seawater velocity u_{wmax} was taken as 0.05 m/s. The submarine crude oil leakage and diffusion conditions were simulated under seawater densities of 1025,1035, and 1045 kg/m^3. The volume fraction of crude oil leakage with different seawater densities is shown in Fig. 6 (cross section of z = 5 m), and the variation in the diffusion height of crude oil in seawater with leakage time is shown in Fig. 7.

Figures 6 and 7 show that the diffusion patterns of crude oil are almost the same under different seawater densities, and the change in seawater density has little

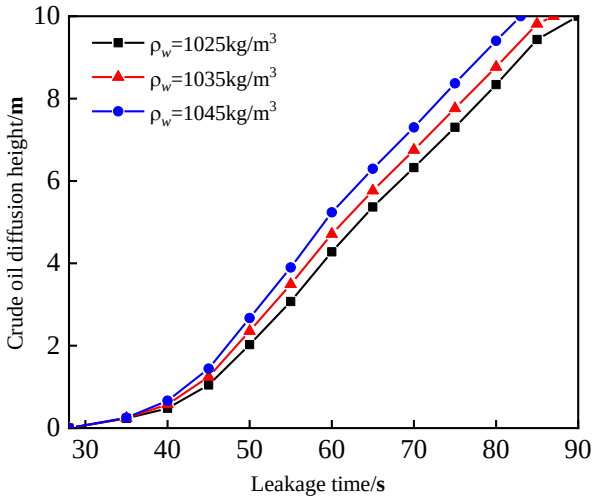

Fig. 7 Variation of diffusion height of crude oil in seawater with leakage time

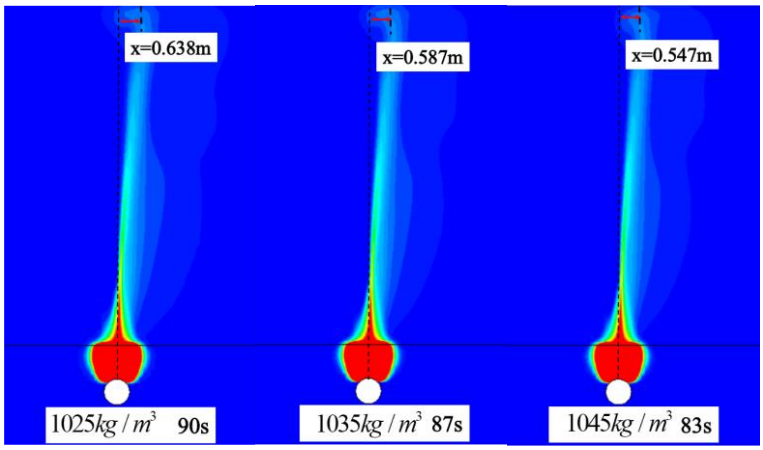

Fig. 8 Transverse diffusion distance of crude oil under different seawater densities

effect on the diffusion law of sea mud. When crude oil diffuses into seawater, the greater the density of seawater, the greater the diffusion rate of crude oil, and the higher the diffusion height at the same time. For example, when the leakage time is 55 s, the diffusion heights of crude oil in seawater at seawater densities of 1025,1035, and 1045 kg/m^3 are 3.068, 3.504, and 3.886 m, respectively. The reason is that the greater the density of seawater, the greater the buoyancy formed by the diffusion of crude oil in seawater, and the greater the upward acceleration generated. Thus, the greater the diffusion speed of crude oil, the shorter the time it takes to spread to the sea surface. A comparison of the transverse diffusion distances x_0 of crude oil at different seawater densities is shown in Fig. 8.

Figure 8 shows that, when the seawater densities are 1025, 1035, and 1045 kg/m3, the transverse diffusion distances of crude oil are 0.638, 0.587, and 0.547 m, respectively — that is, with an increase in seawater density, the transverse diffusion distance of crude oil decreases. The analysis shows that the greater the density of seawater, the greater the diffusion speed of crude oil in seawater, the shorter the time to diffuse to the sea surface, and the shorter the migration distance of crude oil in the horizontal direction (*x*-direction) under seawater entrainment.

3.2 Seawater Velocity

The pipeline buried depth was taken as 0.1 m, the seawater density was taken as 1025 kg/m^3, and the maximum velocities of seawater u_{wmax} (surface velocity of seawater) were 0.05, 0.1, 0.15, 0.25 and 0.35 m/s. The diffusion law of a submarine crude oil pipeline after leakage at different seawater velocities was studied. The distribution of the volume fractions in sea mud and seawater after the leakage of crude oil is shown in Fig. 9.

Figure 9 reveals that there is no obvious difference in the diffusion form and diffusion range of crude oil in sea mud at different seawater velocities. When crude oil leaks into seawater, its diffusion pattern varies significantly with the seawater velocity. The greater the seawater velocity, the greater the diffusion range of underwater crude oil. When the seawater velocity is 0.05 and 0.1 m/s, the diffusion trajectory of the oil is columnar, and the transverse diffusion distance is small. When the seawater velocity increases to 0.15 m/s, the central oil column obviously shifts and the transverse diffusion distance begins to increase. When the seawater velocity increases to 0.25 and 0.35 m/s, the transverse diffusion distance of

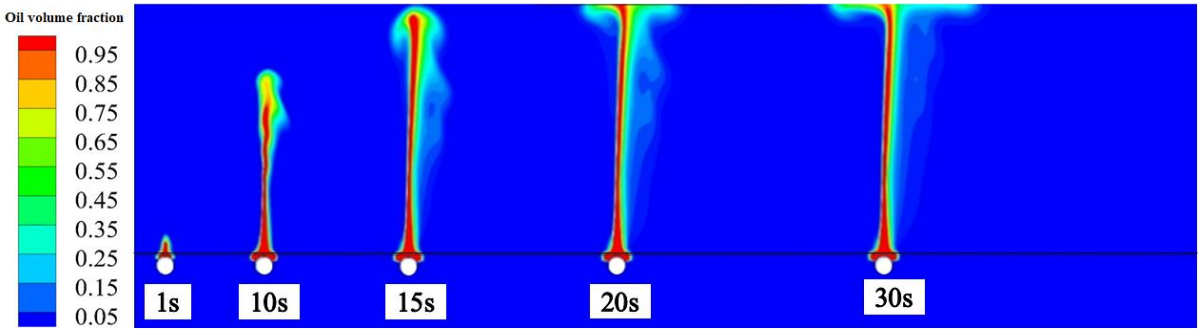

(a) u_{wmax}=0.05 m/s

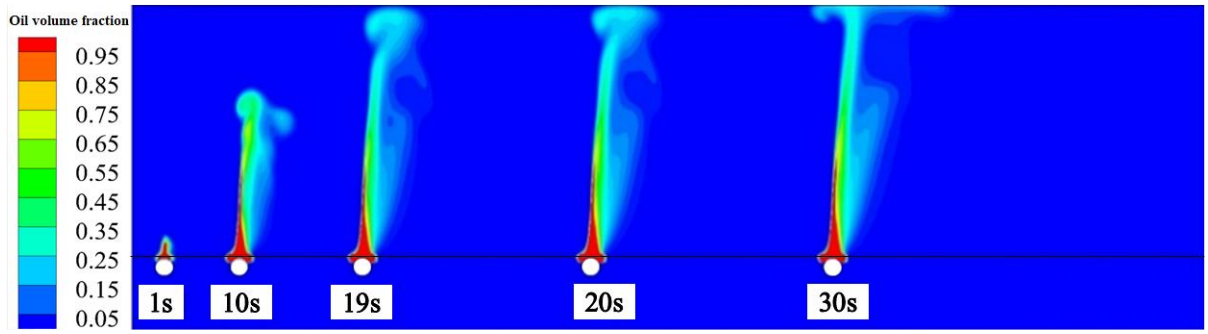

(b) u_{wmax}=0.1 m/s

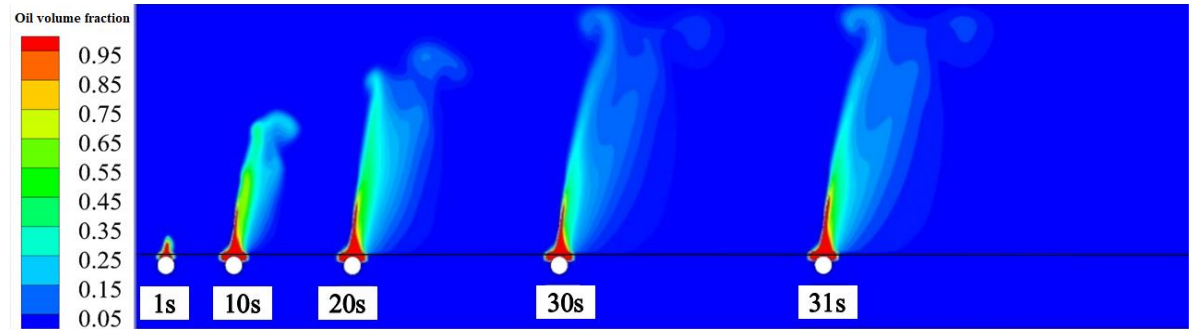

(c) u_{wmax}=0.15 m/s

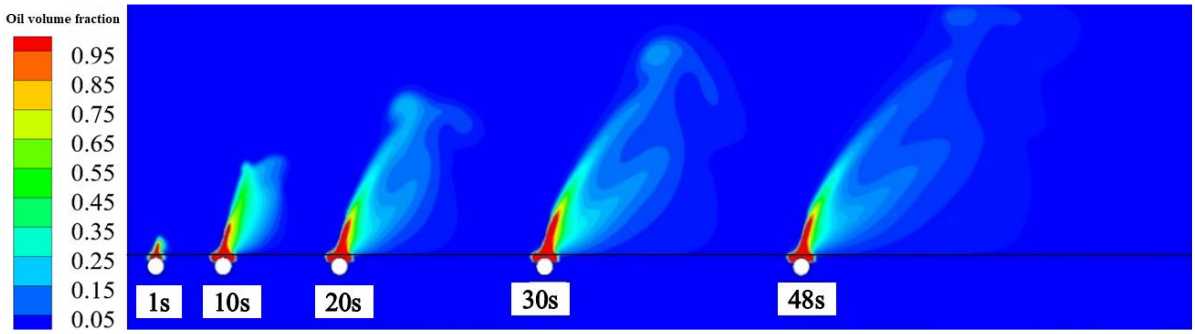

(d) u_{wmax}=0.25 m/s

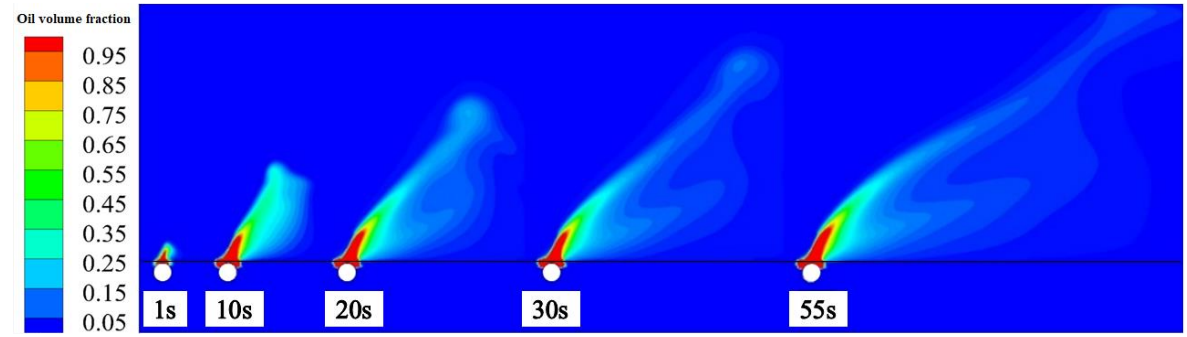

(e) u_{wmax}=0.35 m/s

Fig. 9 Crude oil volume fractions at different seawater velocities

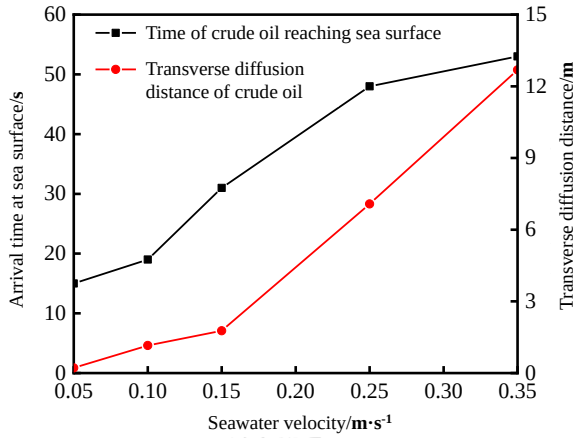

Fig. 10 Relationships between the time of crude oil reaching the sea surface, transverse diffusion distance, and velocity of seawater

the oil increases sharply, the central oil column changed from a columnar to an inclined flame shape, and an oil mass separation trend appears near the sea surface.

As Fig. 10 shows, the greater the velocity of seawater, the longer the time for crude oil to reach the sea surface. When the velocity of the seawater is less than 0.1 m/s, the time for oil to reach the sea surface changes less. When the velocity of the seawater is between 0.1 and 0.35 m/s, the time for the oil to reach the sea surface increases rapidly with the change in the seawater velocity. When the seawater velocity is less than 0.15 m/s, the leakage diffusion range is small, and the transverse diffusion distance of crude oil to the sea surface is less than 2 m. When the seawater velocity is greater than 0.15 m/s, the transverse diffusion distance of the oil to the sea surface increases significantly, the seawater velocity increases to 0.35 m/s, and the transverse diffusion distance of oil to the sea surface increases significantly to 12.693m.

An analysis of the above phenomena shows that the time and transverse diffusion distance of crude oil diffusion to the sea surface increase with an increase in seawater velocity. This is because, when crude oil reaches seawater, it spreads under the action of buoyancy and gravity. A smaller seawater velocity has a less transverse impact on the crude oil, and the rising speed is faster; thus, it can reach the water surface faster. Under a higher seawater velocity, the rising speed is slower, and the time to reach the sea surface increases. With an increase in seawater velocity, the horizontal velocity of crude oil under seawater entrainment increases; thus, the transverse diffusion distance to the sea surface increases.

3.3 Buried Depth of Pipeline

The seawater velocity was taken as 0.05 m/s, and the seawater density was taken as 1025 kg/m^3. Buried depths h of 0.1, 0.7, and 1.3 m were selected for the simulation, and the diffusion law of the submarine crude oil pipeline after leakage at different buried depths was studied. The volume distributions of oil products in sea mud and seawater at different burial depths are shown in Fig. 11.

As Fig. 11 shows, with an increase in the buried depth of the pipeline, the time required for the crude oil leakage to spread to the seawater level clearly increases. A buried depth h of 0.1 m requires 15 s, and a buried depth of 1.3 m requires 115 s, which is approximately 7.67 times that of 0.1 m. Different buried depths have different oil diffusion patterns in the sea mud. When the buried depth is small, the diffusion area in the sea mud is flat and elliptical. With an increase in the buried depth, the short axis of the ellipse gradually lengthens. When the buried depth increases to 1.3 m, the diffusion area of crude oil in the sea mud is vertical and elliptical. When the seawater velocity is 0.05 m/s, there is an oil column in the diffusion of crude oil in seawater. As the buried depth increases, the high- concentration area of the oil column begins to decrease.

An analysis of the oil volume distribution at different buried depths reveals that the diffusion of submarine crude oil pipelines differs significantly at different buried depths. To explore the influence of buried depth further, vector diagrams of oil diffusion velocity in the area above the leakage port from mud to seawater at three buried depths were compared, as shown in Fig. 12. (The area is 1.2 m wide and 1.8 m high, and the location changes according to the buried depth of the pipeline.)

As shown in Fig. 12, the diffusion velocity of crude oil at different buried depths spreads radially, and the overall trend is that it first decreases and then increases at the boundary of the interface of sea mud and seawater (y=0 m). In the same horizontal direction, the velocity at the center line of the leakage hole is the highest. The smaller the buried depth of the pipeline, the greater the diffusion velocity of oil in the sea mud and seawater. When the buried depth is 0.1 m, the main flow type of oil in the sea mud above the pipeline leakage hole is a jet, and only the flow type in the far sea mud is porous flow. In this case, the diffusion velocity of crude oil in water is the highest, reaching approximately 2.5 m / s. When the buried depth is 0.7 and 1.3 m, the speed of the crude oil flowing out of the leakage hole drops sharply, and then it displays seepage movement in the sea mud at a very small speed, reaching approximately 1.5 and 1.0 m/s respectively in the seawater.

In the analysis of the oil volume distribution, it can be seen intuitively from Fig. 11 that the smaller the buried depth, the shorter the time for crude oil to leak to sea level, and the larger the pollution range in the water at the same time. However, the diffusion process of crude oil in sea mud is not obvious compared with that in seawater; therefore, the diffusion ranges of crude oil in sea mud at different buried depths were compared, as shown in Fig. 13.

As Fig.13 shows, the maximum transverse diffusion width of crude oil in sea mud at different buried depths increases with time. When the leakage time is less than 10 s, the leakage diffusion range increases rapidly. When the leakage time exceeds 10 s, the growth trend of the diffusion

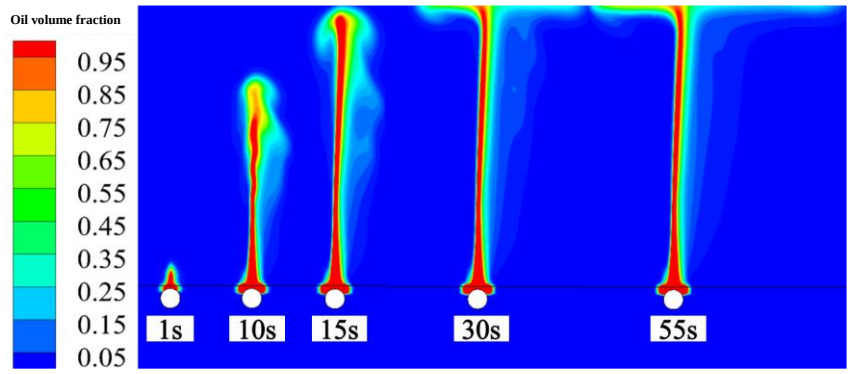

(a) h=0.1 m

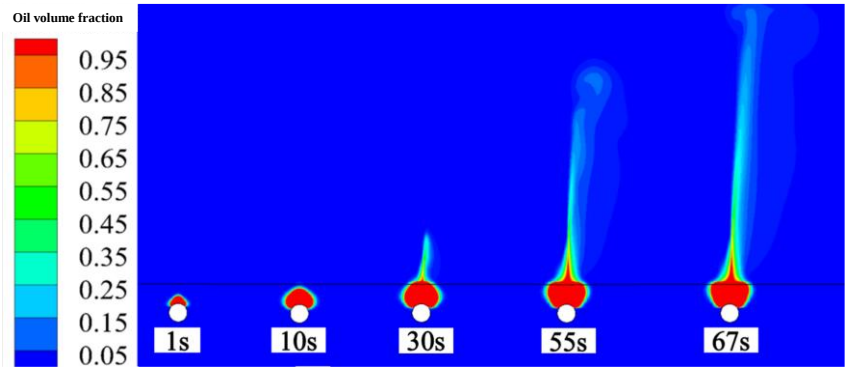

(b) h=0.7 m

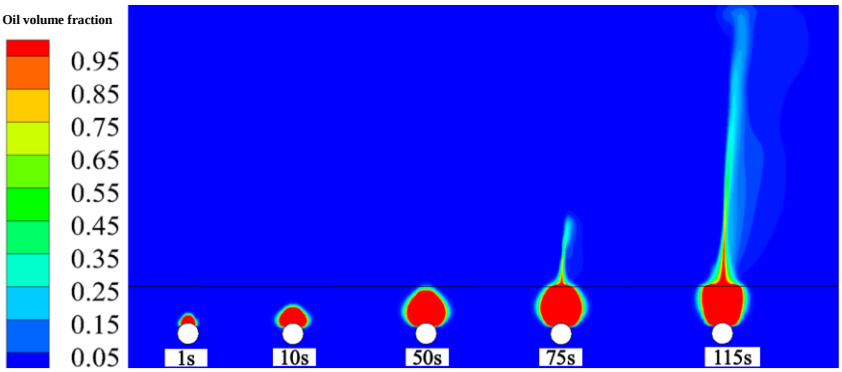

(c) h=1.3 m

Fig. 11 Crude oil volume fractions at different buried depths

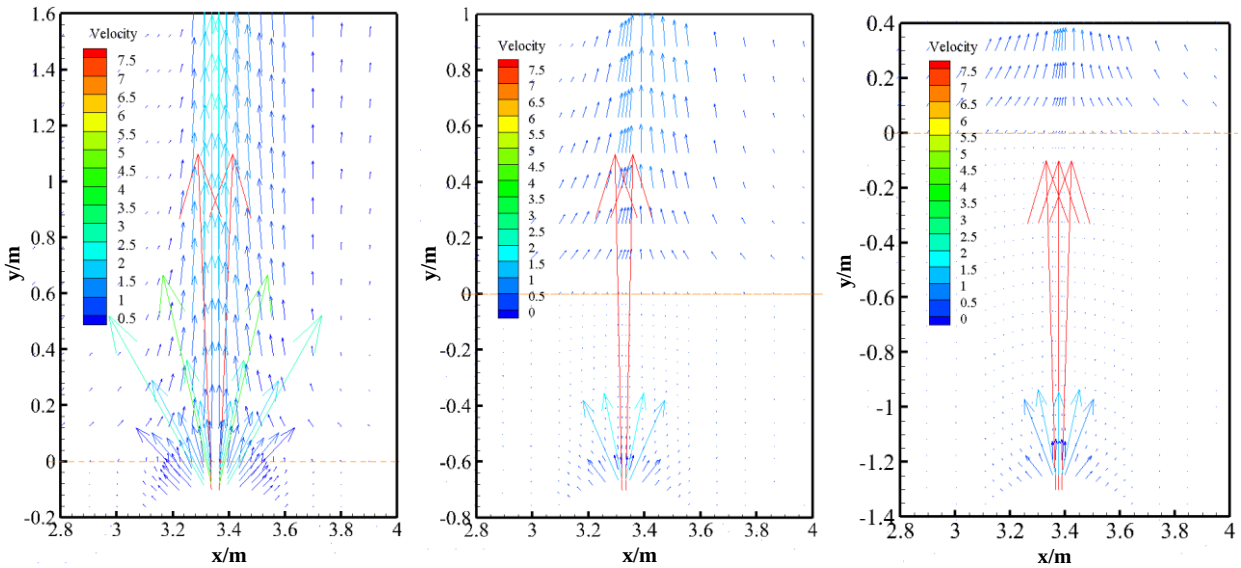

Fig. 12 Vector illustration of oil leakage diffusion velocities at different buried depths

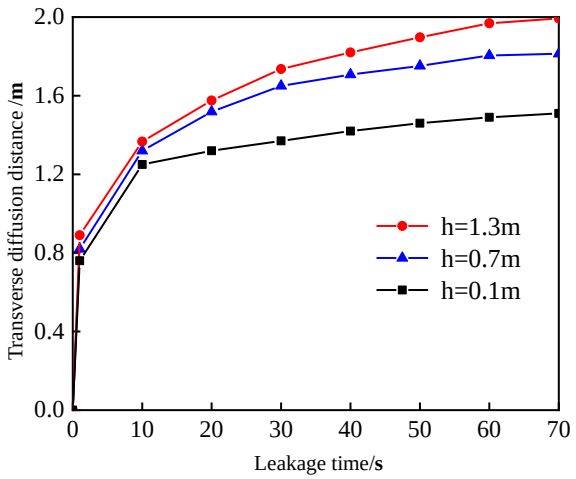

Fig. 13 Variation of transverse diffusion width of crude oil in sea mud at different buried depths

range begins to decrease. After 60 s, the growth trend is slower. With an increase in buried depth, the leakage and diffusion range of crude oil in the sea mud increases. When buried depths are 0.1, 0.7, and 1.3 m, the maximum transverse diffusion widths are approximately 1.51, 1.81, and 2.0 m respectively.

The analysis shows that, when the buried depth is small, the thickness of the sea mud on the upper part of the pipeline is small, which makes the resistance of some sea mud on the pipeline far less than that in the other directions. Therefore, when the buried depth is small, the crude oil moves upward more easily than in the left and right directions. As the buried depth increases, the thickness of the sea mud above the pipeline increases, which makes the sea mud resistance in all directions around the pipeline increasingly uniform. At this time, the moving speed in each direction is more uniform, and the trend of the crude oil moving in the left and right directions increases. Therefore, it is necessary for the oil to move upward. Because the resistance of sea mud in all directions is quite large, and compared with sea mud, crude oil diffuses more easily in seawater. With an increase in time, crude oil continues to leak into the seawater; thus, the longer the leakage time, the slower the increase in the transverse diffusion width and diffusion range of crude oil in sea mud.

3.4 Multiple Linear Regression Analysis

Based on the results of the above simulation of the diffusion of crude oil in sea mud and seawater after leakage from the submarine-buried crude oil pipeline, the analysis shows that the time t of crude oil diffusion to the sea surface and the transverse diffusion distance x_0 of crude oil are mainly related to the seawater velocity u_{wmax}, seawater density ρ_w and pipeline depth h of the submarine pipeline. A multivariate linear regression model is a linear regression model with multiple explanatory variables, that is used to explain the linear relationship between the explanatory variables and other explanatory variables. The prediction equation can be established using multiple linear regression to fit the time of crude oil diffusion to the sea surface and the transverse diffusion distance of crude oil.

The multiple linear regression models are established as

$$t = \alpha_0 + \alpha_1 u_{wmax} + \alpha_2 \rho_w + \alpha_3 h + \varepsilon_0 \tag{15}$$

$$x_0 = \beta_0 + \beta_1 u_{wmax} + \beta_2 \rho_w + \beta_3 h + \varepsilon_1 \tag{16}$$

where α_0 and β_0 are regression constants and α_1, α_2, α_3, β_1 , β_2 , and β_3 are regression coefficients.

The multiple linear regression model is evaluated using the F-statistic, t-statistic, and goodness of fit.

$$SST = \sum_{i=1}^{n} (y_i - \bar{y})^2 \tag{17}$$

$$SSR = \sum_{i=1}^{n} (\hat{y} - \bar{y})^2 \tag{18}$$

$$SSE = \sum_{i=1}^{n} (y_i - \hat{y})^2 \tag{19}$$

$$F = \frac{SSR / p}{SSE / (n - p - 1)} \tag{20}$$

where y is the dependent variable, $\bar{y}$ is the mean of the dependent variable, and $\hat{y}$ is the fitted value. Here, SST is the total sum of squares, SSR is the regression sum of squares, and SSE is the residual sum of squares. In addition, n is the number of sample sizes, and p is the number of independent variables. The P-value of the F-statistic is less than 0.05, indicating that the regression model is significant.

$$t_1 = \frac{\beta_j - \beta_J}{S_e(\beta_j)} \tag{21}$$

$$t_2 = \frac{\alpha_j - \alpha_J}{S_e(\alpha_j)} \tag{22}$$

where S_e is the standard error, and the P-value of the t-statistic is less than 0.05, indicating that each regression coefficient is significant and should be retained in the regression equation.

$$R^2 = SSR / SST \tag{23}$$

The range of R^2 values is (0,1), and the closer the result is to 1, the more significant the regression equation.

The multi-linear regression model established by Python programming was solved. Under the influence of the seawater velocity, seawater density, and pipeline depth, the time of crude oil diffusion to the sea surface and the transverse diffusion distance equation of crude oil are

$$t = 378.6096 + 136.8123 u_{wmax} - 0.369 \rho_w + 83.2649 h \tag{24}$$

$$x_0 = -4.3505 + 41.8664 u_{wmax} + 0.0013 \rho_w + 1.4779 h \tag{25}$$

The P-values of the F-statistic were 7.12e-07 and 9.55e-05, approaching 0. The P-values of the t-statistic were less than 0.05. The R^2 are 0.993 and 0.965

respectively, and the linear relationship is significant. The fitting formula for the time when crude oil diffuses to the sea surface and the lateral diffusion distance of crude oil with seawater velocity, seawater density and pipeline buried depth can accurately predict the best rescue time and crude oil pollution range after the accident, and provide some theoretical support for the formulation of an emergency plan for the leakage of crude oil from buried pipelines.

4. CONCLUSION

The VOF model and porous-medium model were used to simulate the leakage of buried crude oil pipelines on the seabed, and the effects of seawater density, seawater velocity, and pipeline depth on the diffusion of oil leakage were studied. The specific conclusions are as follows.

(1) The floating velocity of crude oil in seawater decreases with the increase in seawater velocity, and the underwater migration time and diffusion range increase accordingly. When the seawater flow rate is greater than 0.10 m/s, the leakage and diffusion forms of oil begin to change significantly. A seawater velocity greater than 0.15 m/s has the greatest impact on the leakage and diffusion of crude oil.

(2) The density of seawater is positively correlated with the diffusion velocity of crude oil at the same height in seawater. It is negatively correlated with the time of crude oil leakage and diffusion to the sea surface and the transverse diffusion distance of crude oil. Compared with a density of 1045 kg/m^3, the transverse distance of a density of 1025 kg/m^3 is increased by 0.091 m, which is approximately 1.166 times that of a density of 1045 kg/m^3.

(3) As the buried depth of the pipeline increases, the leakage and diffusion rates of the oil decrease, the time taken to diffuse to the water surface increases, and the high-concentration area of crude oil in the seawater decreases. The diffusion widths of crude oil in sea mud increase by 20% and 32.5%, respectively, when the buried depth of the pipeline is 0.7 and 1.3 m compared with 0.1 m.

(4) Combined with the simulation data, a multiple linear regression model of the seawater velocity, seawater density, and submarine pipeline buried depth at the time of crude oil diffusion to the sea surface, along with the lateral diffusion distance of crude oil, was established. The model can accurately predict the optimal rescue time for an accident after leakage from a submarine-buried crude oil pipeline and the range of crude oil diffusion pollution.

(5) The simulation of sea mud and seawater was simplified. Researchers interested in this should conduct more in-depth studies. In addition, the study of more influencing factors affecting the crude oil leakage law of submarine-buried pipelines, such as crude oil density and crude oil leakage rate, is needed.

CONFLICT OF INTEREST

The authors have no relevant financial or non-financial interests to disclose.

AUTHORS CONTRIBUTION

X. F. Lv is mainly responsible for putting forward concepts, revising manuscripts, project management and obtaining funds, and can be a correspondent. **H. J. Zhao** is mainly responsible for research methods, data analysis and first draft writing, and can be the first author. **D. Zhang** participated in research methods, data analysis and manuscript revision. Other authors (**L. L. Song**, **J. W. Li**, **F. Chen**, **X. Q. Xie**) helped to organize the manuscript.

REFERENCES

Bonvicini, S., Antonioni, G., & Cozzani, V. (2018). Assessment of the risk related to environmental damage following major accidents in onshore pipelines. *Journal of Loss Prevention in the Process Industries*, *56*, 505–16. https://doi.org/10.1016/j.jlp.2018.11.005.

Fu, H., Yang, L., Liang, H., Wang, S., & Ling, K. (2020). Diagnosis of the single leakage in the fluid pipeline through experimental study and CFD simulation. *Journal of Petroleum Science and Engineering*, *193*, 107437. https://doi.org/10.1016/j.petrol.2020.107437.

Gong, S., Zhang, T., Wang, X., & Liu, C. 2020. Numerical simulation on dynamic behaviour of deepwater J-lay systems. *Ocean Engineering*, *196*, 106771. https://doi.org/10.1016/j.oceaneng.2019.106771.

Guan, L., Liu, D. J., & Zhao, L. (2015). Numerical study on crude oil leakage of semi-buried pipe underwater. *Journal of Liaoning University of Petroleum & Chemical Technology*, *35*(3), 27-30. https://doi.org/10.3969/j.issn.1672-6952.2015.03.007.

Han, L. J., Wang, Q., & Yang, Q. H. (2015). Leak detection and localization analysis of underwater gas pipeline based on distributed fiber optic sensing. *Chinese Journal of Sensors and Actuators*, (7), 1097-1102. https://doi.org/10.3969/j.issn.1004-1699.2015.07.026.

He, G., Liang, Y., Li, Y., Wu, M., Sun, L., Xie, C., & Li, F. (2017). A method for simulating the entire leaking process and calculating the liquid leakage volume of a damaged pressurized pipeline. *Journal of Hazardous Materials*, *332*, 19–32. https://doi.org/10.1016/j.jhazmat.2017.02.039.

Ji, J., Li, Y. X., & Ji, J. (2018）. Comparison between the pipeline leakage detection technologies based on optical fiber sensing. *Oil & Gas Storage and Transportation*, *37*(4), 368-377. https://doi.org/10.6047/j.issn.1000-

8241.2018.04.002

Kotzakoulakis, K., & George, S. C. (2018). Predicting the weathering of fuel and oil spills: A diffusion-limited evaporation model. *Chemosphere*, *190*, 442–53. https://doi.org/10.1016/j.chemosphere.2017.09.142.

Lin, M. H., He, G. X., & Li, Y. S. (2017). A Numerical simulation on the spilled oil diffusion of submarine pipelines. *Journal of Beijing Institute of Petro-chemical Technology*, *25*(4), 83-90. https://doi.org/10.12053/j.issn.1008-2565.2017.04.015.

Liu, G. (2015). Research on leak detection of submarine oil pipeline and simulation technology of oil spill diffusion [Master Thesis]. *Chengdu: Southwest Petroleum University*.

Liu, K. R., Wu, M., & Wang, T. X. (2012). Numerical simulation on leakage and diffusion of submarine buried hot oil pipeline. *Journal of Safety Science and Technology*, *8*(8), 63-68. https://doi.org/10.3969/j.issn.1673-193X.2012.08.011.

Lu, S. G., Zhang, J., & Wu, S. J. (2018). Experiments and numerical simulation on the horizontal leakage of submarine pipelines. *Oil & Gas Storage and Transportation*, *37*(4), 469-474. https://doi.org/10.6047/j.issn.1000-8241.2018.04.017.

Mark, R., Per D., & Alun, L. (2004). Modelling of dispersant application to oil spills in shallow coastal waters. *Environmental modelling & software*, *19*(7/8), 681-690. https://doi.org/10.1016/j.envsoft.2003.08.014

Manda, U., Parahovnik, A., & Peles, Y. (2022). Thermoacoustic waves and Piston Effect inside a microchannel with Carbon Dioxide near critical conditions. *Thermal Science and Engineering Progress*, *36*. https://doi.org/10.1016/j.tsep.2022.101528.

Manda, U., Parahovnik, A., & Peles, Y. (2020). *Theoretical investigation of boundary layer behavior and heat transfer of supercritical carbon dioxide (sCO2) in a microchannel*. 2020 19th IEEE Intersociety Conference on Thermal and Thermomechanical Phenomena in Electronic Systems (ITherm), Orlando, FL, USA. https://doi.org/10.1109/ITherm45881.2020.9190408.

Manda, U., Peles, Y., & Putnam, S. (2021). *Comparison of heat transfer characteristics of flow of supercritical carbon dioxide and water inside a square microchannel*. 2021 20th IEEE Intersociety Conference on Thermal and Thermomechanical Phenomena in Electronic Systems (iTherm), San Diego, CA, USA. https://doi.org/10.1109/ITherm51669.2021.9503192.

Manda, U., Parahovnik, A., Mazumdar, S., & Peles, Y. (2023). Heat transfer characteristics of turbulent flow of supercritical carbon dioxide (sCO2) in a short-heated microchannel. *International Journal of Thermal Sciences*, *192*, A. https://doi.org/10.1016/j.ijthermalsci.2023.108389.

Neofytou, P., Venetsanos, A. G., & Vlachogiannis, D. (2006). CFD simulations of the wind environment around an airport terminal building. *Environmental modelling & software*, *21*(4), 520-524. https://doi.org/10.1016/j.envsoft.2004.08.011

Papadimitrakis, J., Psaltaki, M., & Christolis, M. (2006). Simulating the fate of an oil spill near coastal zones: The case of a spill (from a power plant) at the Greek Island of Lesvos. *Environmental modelling & software*, *21*(2), 170-177. https://doi.org/10.1016/j.envsoft.2004.04.020

Shi, L., Ma, G. Y., & Wang, X. (2014). Numerical study on crude oil leakage of underwater buried pipeline. *Contemporary Chemical Industry*, (1), 153-155. https://doi.org/10.3969/j.issn.1671-0460.2014.01.058.

Sun, Y., Cao, X. W., & Liang, F. C. (2019). Investigation on underwater spreading characteristics and migration law of oil leakage from damaged submarine pipelines. *Process Safety and Environmental Protection*, *127*, 329-347. https://doi.org/10.1016/j.psep.2019.05.030.

Wang, Q., Shi, W., & Yu, X. (2018). Influence of different water flow speed on the oil spill of submarine pipeline. *Contemporary Chemical Industry*, *47*(7), 1460-1463. https://doi.org/10.3969/j.issn.1671-0460.2018.07.040.

Wei, Z. Y., Zhu, X. L., & Guo, Q. W. (2018). Numerical simulation of process of oil spill from damaged submarine pipeline based on CFD. *Journal of Hefei University of Technology*, *41*(07), 002-1008. https://doi.org/10.3969/j.issn.1003-5060.2018.07.025.

Wols, B. A., Hofman, J. A. M. H., & Uijttewaal, W. S. J. (2010). Evaluation of different disinfection calculation methods using CFD. *Environmental modelling & software*, *25*(4). https://doi.org/10.1016/j.envsoft.2009.09.007

Yang, Y. P., Wu, G.X., & Liu, G. S. (2016). Features of self-embedding technology of spoiler and operation analysis of submarine pipeline in Hangzhou Bay. *Journal of Marine Sciences*, *34*(3), 57-61. https://doi.org/10.3969/j.issn.1001-909X.2016.03.009.

Zhang, B. Z., Kang, R. X., & Zhu, H. Q. (2022). Numerical simulation and safety evaluation of multi-source leakage of buried product oil pipeline. *Energy Sources, Part A: Recovery, Utilization, and Environmental Effects*, 6737-6757. https://doi.org/10.1080/15567036.2022.2100518.

Zhang, Y. G., Lan, H. Q., & Fu, Z. D. (2015). Leakage intensity testing model of the underground oil-refining pipes and its experimental verification. *Journal of Safety and Environment*, *15*(2), 134-137. https://doi.org/10.13637/j.issn.1009-6094.2015.02.029

Zhu, H. J., You, J. H., & Zhao, H. L. (2017a). Underwater spreading and surface drifting of oil spilled from a submarine pipeline under the combined action of wave and current. *Applied Ocean Research*, 64, 217-235. https://doi.org/10.1016/j.apor.2017.03.007

Zhu, H. J., You, J. H., & Zhao, H. L. (2017b). An experimental investigation of underwater spread of oil spill in a shear flow. Marine Pollution Bulletin, s116 (1-2), 156-166. https://doi.org/10.1016/j.marpolbul.2017.01.002

Zhu, H. J., Lin, P. Z., & Qian, P. (2014). A CFD (computational fluid dynamic) simulation for oil leakage from damaged submarine pipeline. *Energy*, *64*(1), 887–899. https://doi.org/10.1016/j.energy.2013.10.037

APPENDIX

The UDF code that represents the seawater velocity at the seawater inlet is

```
#include"udf.h"
#define h 10
#define um 0.5
DEFINE_PROFILE(inlet,t,i)
{
real x[ND_ND];
real y;
face_t f;
begin_f_loop(f,t)
{
F_CENTROID(x,f,t);
y=x[1];
F_PROFILE(f,t,i)=-(um/h*h)*pow(y-h,2)+um;
}
end_f_loop(f,t)
}
```